Determination of the Crosslink Density of Tire Tread Compounds by Different Analytical Methods

Crosslink density · swelling · TSSR · thiol-amine-method · ^{1}H NMR relaxation · Mooney-Rivlin · DFM

The crosslink density of rubber compounds influences the in-rubber properties of the final product to a great extent. There are several analytical methods available to determine this crosslink density like equilibrium swelling experiments, Temperature Scanning Stress Relaxation (TSSR) measurements, thiol-amine-method, ^{1}H NMR relaxation, stress-strain analysis according to Mooney-Rivlin or to a non-Gaussian tube model of rubber elasticity (dynamic flocculation model, DFM). SSBR/BR model compounds filled with a Silica/Silane system were produced with varying amounts of accelerator and sulfur and investigated with these different analytical methods. The evaluation shows that methods like DFM, TSSR and Mooney-Rivlin correlate very well but that the thiol-amine method is unsuitable for these silica-filled compounds.

Bestimmung der Vernetzungsdichte an Reifenlaufflächen-Materialien mit verschiedenen analytischen Methoden

Vernetzungsdichte · Quellung · TSSR · Thiol-Amin-Methode · ^{1}H NMR Relaxation · Mooney-Rivlin · DFM

Die Vernetzungsdichte von Gummiproben beeinflusst entscheidend die Gummieigenschaften. Es existieren zahlreiche analytische Methoden wie die Quellungsmethode, die „Temperature Scanning Stress Relaxation“ (TSSR), die Thiol-Amin-Methode, die ^{1}H-NMR-Relaxation, Zug-Dehnungsmessungen gemäß Mooney-Rivlin und das „Non-Gaussian tube“ Modell der Gummielastizität (Dynamisches Flokkulationsmodell, DFM), um die Vernetzungsdichte zu bestimmen. Es wurden Silica/Silan gefüllte SSBR/BR Modellmischungen mit unterschiedlichen Beschleuniger- und Schwefelgehalten hergestellt und mit diesen analytischen Methoden untersucht. Die Auswertung zeigt, dass die DFM, TSSR und Mooney-Rivlin Methoden sehr gut miteinander korrelieren, dass aber die Thiol-Amin Methode für diese Silica-gefüllten Mischungen ungeeignet ist.

Figures and Tables: By a kind approval of the authors.

Introduction

The crosslink density influences mainly the final in-rubber properties of rubber compounds. The most common way of elastomer curing is based on the use of accelerated sulfur curing systems. Charles Goodyear and Thomas Hancock discovered this ability of sulfur to form chemical bonds between polymer chains. [1-4] Sulfur curing made the dimensions of elastomer products more stable in a wide range of temperatures and conditions, and improved numerous physical and chemical properties. Further development in the elastomer technology was stimulated by use of curing accelerators. [5]

These organic components served to shorten the curing time and additionally improve the properties. Accelerated sulfur curing is a complex process, different ionic and radical mechanisms are proposed. Despite differences in the detailed explanations, there is a general agreement about the basic steps, as proposed by Morrison and Porter [6] (Fig. 1). During the curing process, one of the critical steps is the formation of polysulfidic accelerator-terminated pendant groups (RSyAcc) which are bound to the polymer chains. In further reactions, they recombine with other pendant groups or directly with the polymer chains. [7,8] In this way, intermolecular crosslinks are formed, which connect the chains. The number of crosslinks per unit volume in a polymer network is called crosslink density (CLD). [9] Since intermolecular crosslinks are elastically effective, they influence to a very high extent multiple properties of the elastomeric material (Fig. 2). [10,11]

The CLD is a basic structural parameter characterizing the polymer networks. Crosslinks can have various structures. Short, rigid bonds created directly between polymer chains are carbon-carbon (C-C) crosslinks which were formed when a radical process takes place. Sulfidic crosslinks are longer and consist of sulfur atoms incorporated between the polymer chains. Depending on the number of these atoms, they are classified as monosulfidic (C–S–C), disulfidic (C–S_2–C) and polysulfidic (C–S_x–C, x ≥ 3) crosslinks (Fig. 3).

Since all these crosslinks have different structures and length, they show different characteristics. The type of crosslinks is another structural parameter, which strongly influences the behavior of the polymer chains and resulting properties of the material. [12,13] Recently, Bandzierz showed the importance of intramolecular crosslinks and their influence on in-rubber properties. [14] All in all, the density and type of crosslink should be carefully adjusted in accordance with the required in-rubber properties. Considering e.g. modern passenger car tire tread formulations where the rubber is filled with a Silica/Silane system, additional crosslinks have to be considered: the silica – silane – polymer bonds. [15] There is up to now no analytical method available which can distinguish between sulfur bridges between two polymer molecules or between a hydrophobized silica and a polymer. Therefore, the term “crosslink density” describes in the following the sum of both contributions.

There are different methods described in the literature to detect crosslink density, based on different physical or chemical phenomenon (Fig. 4). The different methods are described in detail in the following.

Mooney-Rivlin

The Mooney-Rivlin theory [16, 17] is based on an entropy elastic deformation behavior. It was developed empirically from J. Mooney and R.S. Rivlin due to describe the crosslinks and entanglements inside an unfilled compound (Fig. 5).

Authors

Anke Blume, Jens Kiesewetter, Evonik Resource Efficiency, Wesseling, Germany

Corresponding Author:
Prof. Dr. Anke Blume
Evonik Resource Efficiency GmbH
Brühler Straße 2
D-50389 Wesseling
E-Mail: anke.blume@evonik.com

KGK RUBBERPOINT

Discover more interesting articles and news on the subject!

www.kgk-rubberpoint.de

Entdecken Sie weitere interessante Artikel und News zum Thema!

1

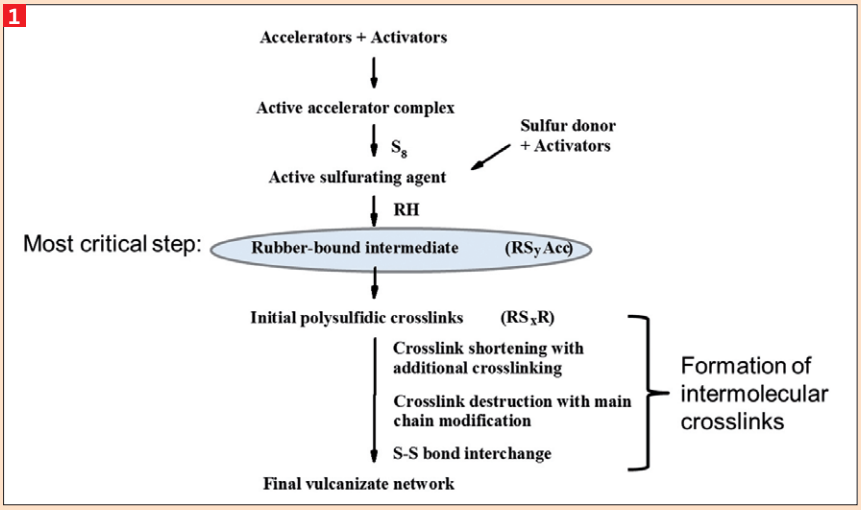

Fig. 1: Reaction scheme for the accelerated sulfur curing of diene rubbers ("R" represents the rubber chain; "Acc" the accelerator moiety) [6].

2

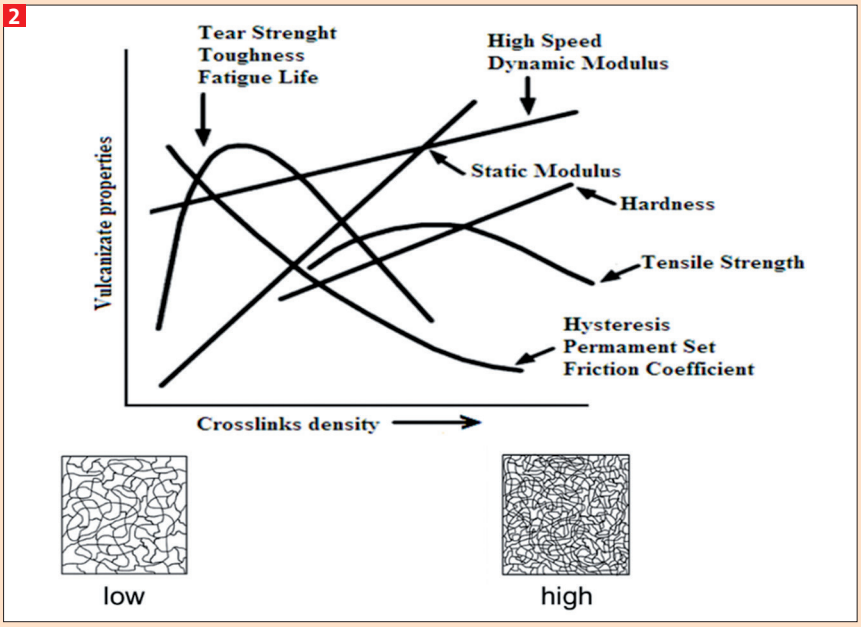

Fig. 2: Influence of the crosslink density on the in-rubber properties [10,11].

3

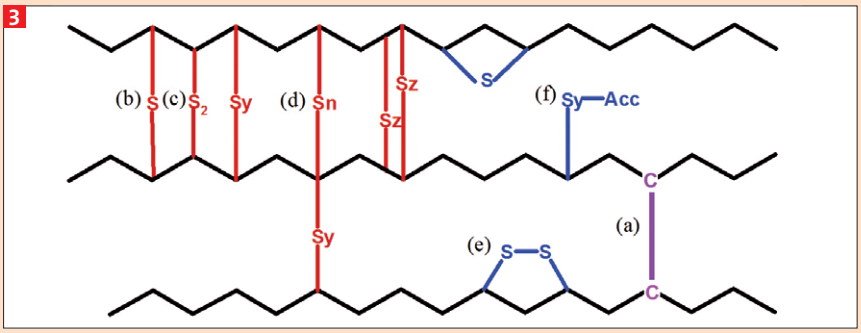

Fig. 3: Network structure and structures formed as a result of accelerated sulfur curing - intermolecular crosslinks: (a) carbon-carbon crosslink; (b) monosulfidic crosslink (C–S–C); (c) disulfidic crosslinks (C–S_2–C); (d) polysulfidic crosslink (C–Sy–C or C–Sz–C, y, z ≥ 3); - intramolecular modifications of the polymer chains: (e) cyclic sulfidic structure; (f) pendant sulfidic group terminated with accelerator moiety. [14].

For filled compounds an energy elastic deformation behavior is present. To determine the CLD of filled compounds, ten stress-strain cycles are required. During the first nine cycles, the destruction of the filler-filler network occurs, which is indicated by a decrease in the Payne-effect. The remaining contribution is the polymer network after this treatment. During the 10th cycle the evaluation according to Moony-Rivlin was carried out. Now the filler-filler network is destroyed but it should be considered that the intrinsic strain of polymer inside the compound is higher than for unfilled compounds. Therefore, λ should be replaced by Λ, the reinforcing factor:

$$\Lambda = \varepsilon \cdot x + 1 \qquad \text{(eq 1)}$$

with ε: strain (relative)

and x: empirical reinforcing factor (theory of Einstein-Guth-Gold, only valid for liquids!)

$$x = 1 + 2{,}5\ vf + 14{,}1\ vf^2 \qquad \text{(eq 2)}$$

with vf: volume filler.

Equilibrium Swelling

The driving force for the analysis of the CLD by swelling, is the mixing entropy. The principle of this measurement is shown in Fig. 6.

The samples of approx. 0,05 g were swollen to equilibrium in toluene for four days at room temperature (23°C ± 1°C). This was followed by drying the samples to a constant weight for four days at 60°C in a Heraeus (Germany) oven with an air circulation system. The crosslink density was calculated based on the Flory-Rehner equation (eq. 3):

$$\nu = -\frac{ln(1 - V_r) + V_r + \chi V_r^2}{V_0 \left(V_r^{\frac{1}{3}} - \frac{2V_r}{f} \right)} \qquad \text{(eq 3)}$$

where:
ν – crosslink density per unit volume in mol/cm³;
V_r – volume fraction of rubber in a swollen sample;
V_0 – solvent molar volume (for toluene: V_0 =106,9 in cm³/mol);
f – functionality of crosslinks (f = 4, assuming the formation of tetra-functional crosslinks);
χ – Flory-Huggins rubber-solvent interaction parameter (for the SBR-toluene system: χ = 0,378 [19].

Thiol-Amine Method

This method allows the differentiation between poly- di- and monosulfidic crosslinks by selective cleavage of bonds. It was originally developed for unfilled polymers [13].

Firstly, the determination of the overall crosslink density is analyzed by swelling experiments: 0,2 g vulcanizate is swollen in 20 ml toluene at room temperature. If an equilibrium of the swelling is reached, which is proven gravimetrical, the overall crosslink density is calculated based on the Flory-Rehner equation (see above). This time, the Flory-Huggins parameter for SBR where considered as 0,31, that for 1,4 cis BR as 0,36 according to Fwata. [20]

Secondly, the vulcanizate is treated with i-propanethiol (0,4 M) in a mixture of piperidine (0,4 M) / heptane for two hours at room temperature under N_2. After the reaction, the sample is washed with petrol ether and dried. The remaining crosslink density is evaluated following the above described swelling procedure. It is assumed that all polysulfidic bridges are broken, the resulting crosslink density is the sum of S_1 and S_2. The difference from the overall crosslink density and this evaluated crosslink density is the amount of polysulfidic bridges.

Finally, another piece of vulcanizate is treated by hexanethiol (1,0 M) in piperidine for two days under vacuum. After the reaction, the sample is washed with petrol ether and dried. The remaining crosslink density is evaluated following the above described swelling procedure. It is assumed that all poly- and disulfidic bridges are broken by this procedure, only the S_1 bridges are remaining. Therefore, the difference between the polysulfidic bridges and this crosslink density is the amount of S_2 bridges.

A relative measurement error of ± 5% is assumed.

Dynamical Flocculation Modell (DFM)

The DFM was developed to describe the stress-strain behavior of filled elastomer compounds [21]. It is based on physical assumptions and models. The behavior of the polymer matrix is described by the non-affine tube model and contains the following assumptions:

- Finite strain of polymer
- Entanglements and network nodes are both important
- (trapped entanglements act as additional junctions)
- Polymer-filler interaction is described by a reinforcing factor:
- Stiff filler particles increase microscopic strain compared to macroscopic strain (hydrodynamic effect)
- Stiff filler aggregates break with increasing strain – reinforcing factor decreases = strain softening
- Broken aggregates re-aggregate with decreasing strain as soft filler aggregates
- Soft filler aggregates react elastically by the next increasing strain, store energy until they break at critical strain, and finally dissipate their energy

There are seven fit parameters which were considered:

- Modulus of the entanglements G_e/ MPa: elastic contribution of polymer entanglements
- Modulus of the network nodes G_c/ MPa: elastic contribution of the network nodes

4

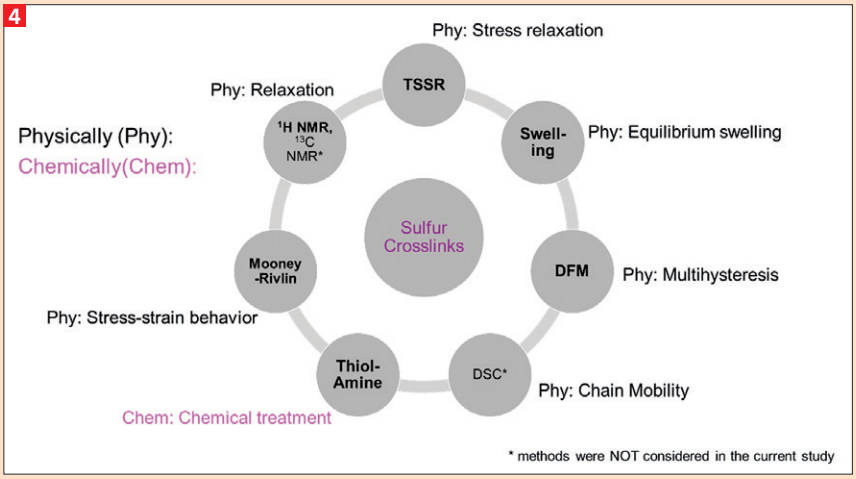

Fig. 4: Different analytical methods to detect sulfur crosslinks.

5

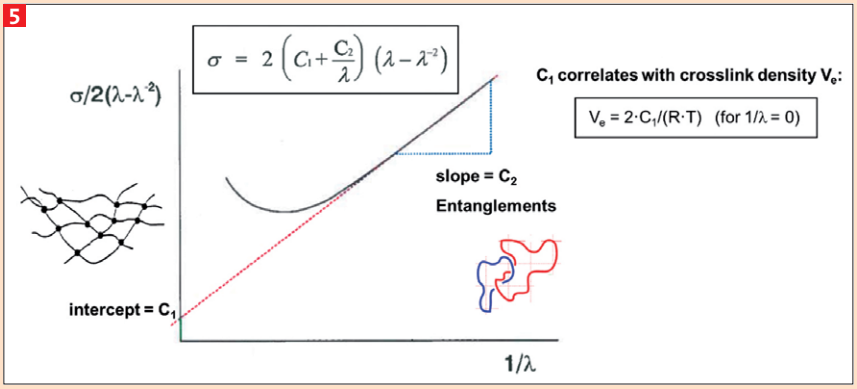

Fig. 5: Determination of the crosslink density by the Mooney-Rivlin approach.

6

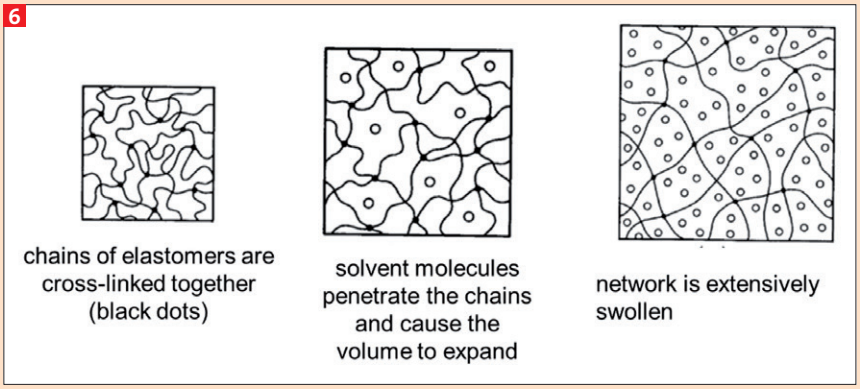

Fig. 6: Scheme of the equilibrium swelling analysis for the determination of the CLD [18].

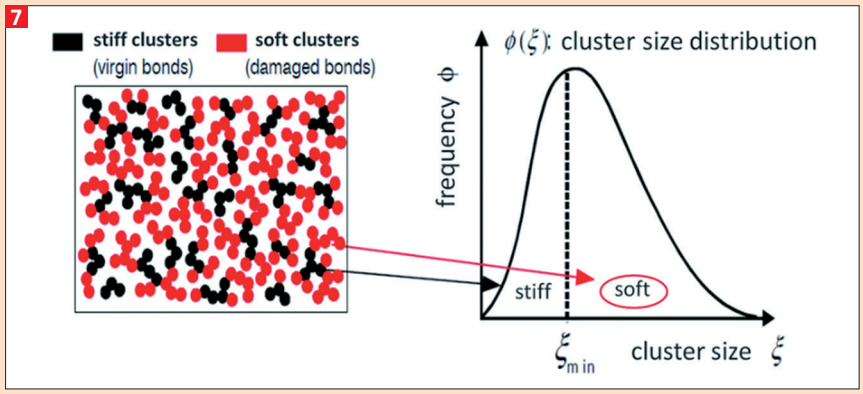

Fig. 7: Model of stiff and soft clusters inside the DFM theory [21].

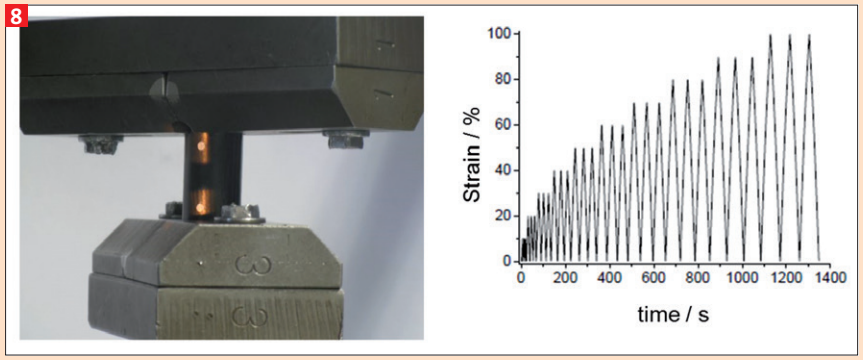

Fig. 8: Left: reflexion points of the samples tested in Zwick 1445; Right: Multihysteresis measurement [21].

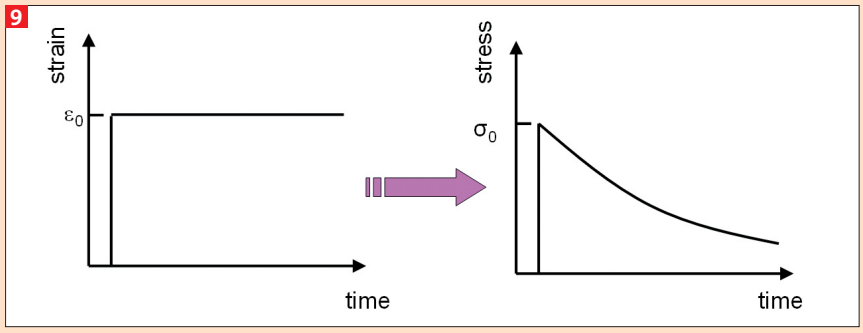

Fig. 9: Principle of stress relaxation [22].

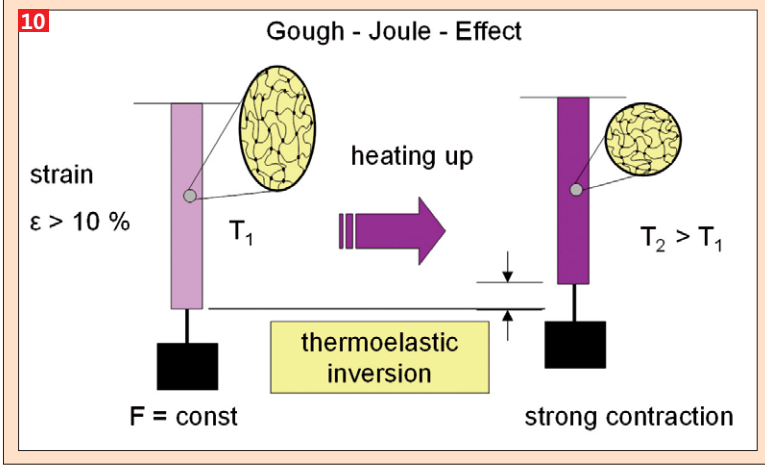

Fig. 10: Principle of thermoelastic inversion.

- Finite strain n: measure for distance of two entanglements or network nodes
- Strength soft bonds s_d/MPa: bond strength of the weak filler cluster (responsible for hysteresis)
- Strength stiff bonds s_v/MPa: bond strength of the stiff filler cluster (responsible for strain softening)
- Medium relative cluster size x_0 (relative with regard to primary particle size)
- Effective filler volume fraction ϕ_{eff}: volume ratio of the active filler

From each sample three dumbbells were prepared. 15 min were added to the regular vulcanization time due to the thickness of the sample. The curing was carried out at 165°C at 200 bar. The Multihysteresis Test was carried out using a Zwick 1445 (Fig. 8, left). The measurement protocol was received by using a speed of 50 mm / min including three cycles at 10%, 20%, 30%, ... , 90%, 100% strain (Fig. 8, right).

TSSR

Another possibility to detect the CLD is the evaluation of the stress relaxation behavior of rubber samples. Usually, the stress is decreasing over the time at constant strain caused by physical and/or chemical processes (Fig. 9). [22]

Normally, such kind of tests are carried out isothermally. The Temperature Scanning Stress Relaxation (TSSR) measurements uses the principle of non-isothermal relaxation behavior. For stresses larger than a threshold (approximately 10%) a thermoelastic inversion is given. This means that for a constant strain an increase in the temperature leads to a strong increase in stress. [23] Entropy elasticity becomes now more important. Figure 10 illustrates this behavior.

In accordance to the classical rubber theory for unfilled compounds the Neo-Hookean law (eq. 4) is valid and the stress σ is proportional the crosslink density of the network V_e. [18, 24, 25]

$$\sigma = V_e \cdot R \cdot T(\lambda - \lambda^2) \qquad \text{(eq 4)}$$

Where R is the universal gas constant, T is the temperature and λ (strain ratio) = l/l_0, with l = length of the sample and l_0 = initial length of the sample.

The temperature coefficient κ of stress for a constant λ is given by equation 5:

$$\kappa = \left(\frac{d\sigma}{dT}\right)_\lambda = V_e \cdot R(\lambda - \lambda^{-2}) \qquad \text{(eq 5)}$$

thus, crosslink density is explained by equation 6.

$$V_e = \frac{\kappa}{R(\lambda - \lambda^{-2})} \qquad \text{(eq 6)}$$

To enlarge this model to filled rubber compounds λ is replaced by Λ and the reinforcing factor x is introduced (eq 7). [26, 27]

$$\Lambda = \varepsilon \cdot x + 1 \qquad \text{(eq 7)}$$

Where ε is the relative strain and the reinforcing factor is determined by $x = 1 + 2{,}5\ v_f + 14{,}1\ v_f^2$ with vf = volume fraction of the filler.

The determination of the thermo-elastic property at constant strain leads to the following stress-temperature cure (Fig. 11). The slope of these curves correlates with the crosslink density.

The non-isothermal tests were carried out in a temperature scanning stress relaxation test device (Fig. 12) made by Brabender GmbH. [28]

The test specimens (dumbbell 2) were placed stress-free in two specimen holders that are then pulled apart to a specific distance. The nominal extension ratio is calculated from the clamps' initial distance and their final distance. After a holding time of two hours the temperature of the specimen is raised linearly at a constant heating rate of 2 K / min from 23°C at the start to a final temperature of 220°C. As a result, the stress over temperature is detected. In addition, a temperature dependent relaxation spectrum is calculated in first approximation (see Fig. 13).

First results described in the literature [28] showed that the determination of crosslink density of unfilled S-SBR compounds with different sulfur contents by TSSR leads to appropriate results (see Fig. 14). Investigations of the repeatability showed a standard deviation of ± 6,6%. Two different evalution methods exist: one according to Brabender and a further developed one according to Heinz [22].

^{1}H NMR

The basis for the determination of the overall network density by using ^{1}H NMR relaxation measurements (Fig. 15) is the molecular dynamic of "C-H-bonds". This method evaluates the molecular dynamic of the hydrocarbons by detecting the transversal molecular nuclear spin relaxation time (T_2) of the ^{1}H atoms of the hydrocarbons.

11

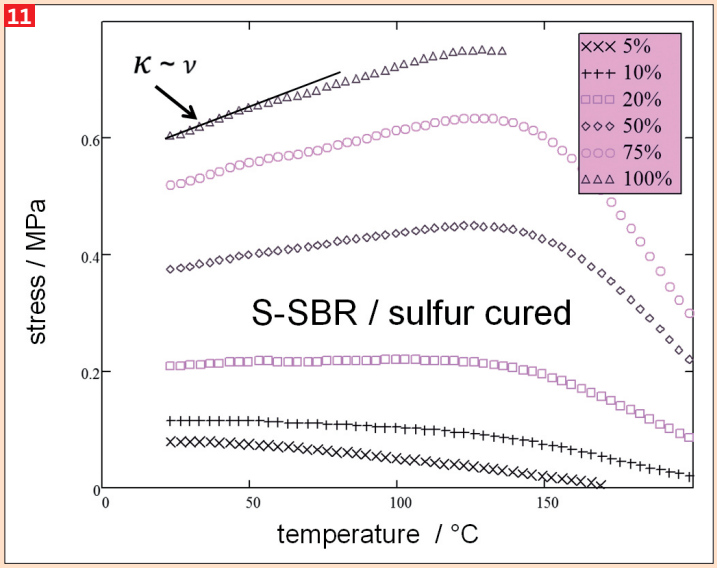

Fig. 11: Stress over temperature for different constant strains.

12

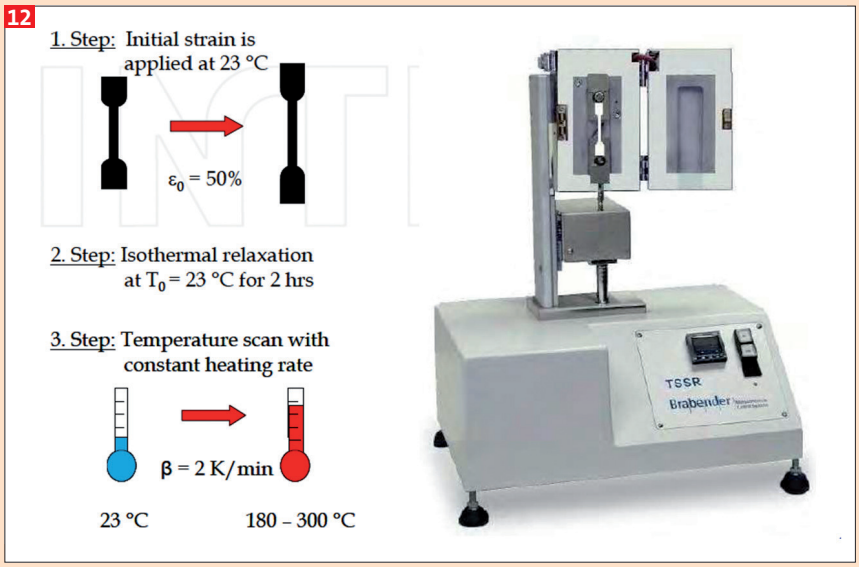

Fig. 12: Test device for TSSR measurements [28].

13

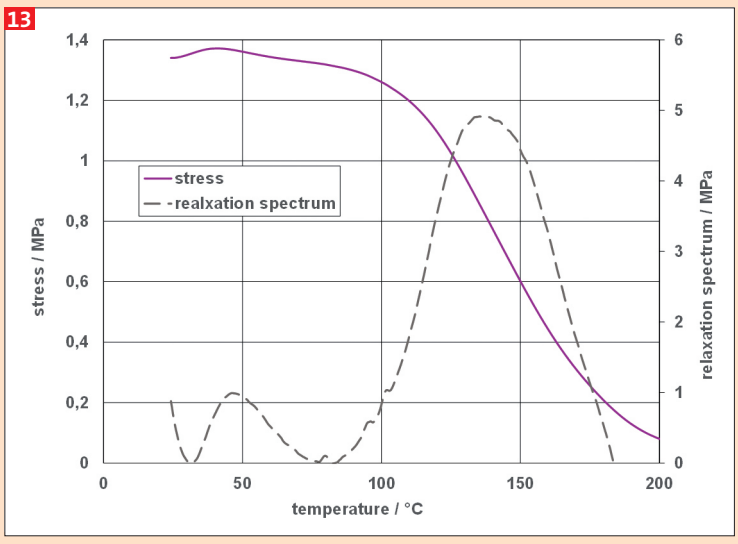

Fig. 13: Typical TSSR curve and temperature depend relaxation spectrum [29].

14

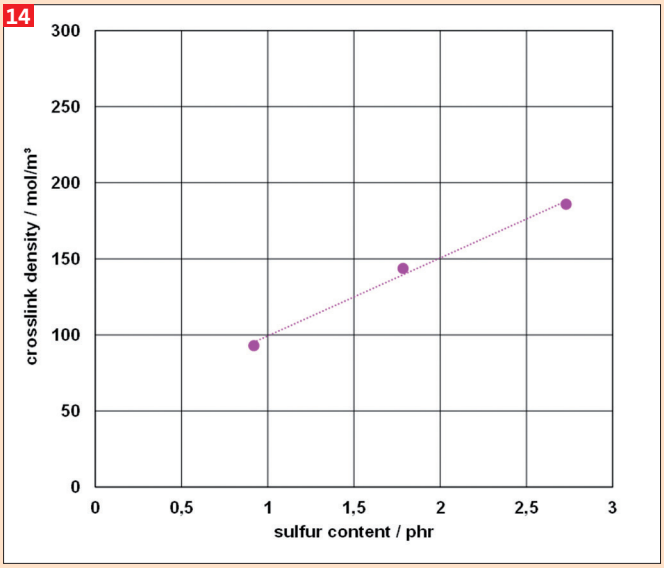

Fig. 14: Crosslink density detected by TSSR dependent on sulfur content [29].

15

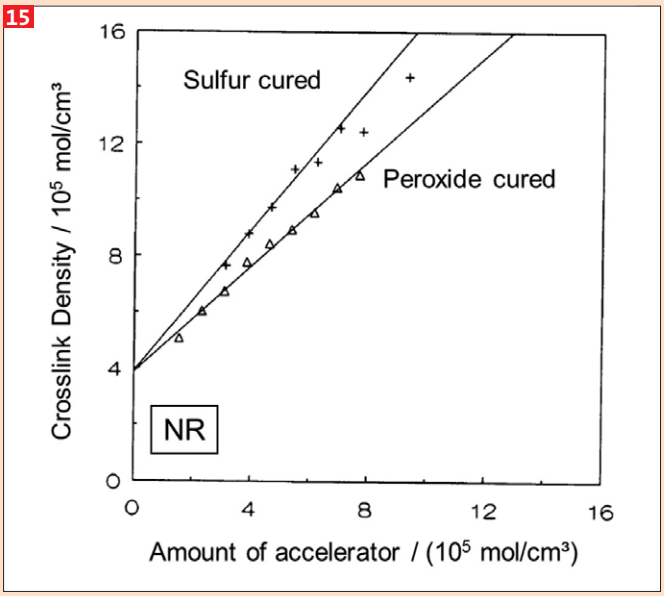

Fig. 15: Determination of Crosslink Density by ^{1}H NMR [30].

1 Green Tire tread compounds

Stage 1	
S-SBR (Buna VSL 4526-2)	96,5
BR (Buna CB 24)	30
ULTRASIL® 7000 GR	80
Si 266™	5,8
Carbon Black: N 330	5
ZnO	2
Stearic acid	1
Oil: Vivatec 500	8,75
Vulkanox HS/LG	1,5
Vulkanox 4020L/G	2
Protektor G 3108	2
DPG 80	2,5

Stage 2	
Batch Sateg 1	
Stage 3	
Batch stage 2	
CBS	variable
sulfur	variable

resulting in very different crosslink densities (CLD)

The transversal relaxation properties of the ^{1}H atoms are only determined by the relative slow movement of the hydrocarbon chain and of the dipolar magnetic interaction of the ^{1}H atoms. The relaxation time T_2 describes the decay of the nucleus magnetization vertical to the static magnetic field after a Hahn-Echo-stimulation (90° - τ - 180°) of the nuclear spins. The intensity of the signal decreases due to physical interactions inside the sample. The relaxation processes are caused by the molecular dynamic which includes slow movements of chain segments. They depend on the microstructure of the polymer, of the physical and chemical crosslinks and on the interaction of polymers with additives and fillers. If the decrease follows a bi-exponential order a detailed evaluation of the polymer dynamics is possible.

The following parameters were used for the crosslink density spectrometer XLDS-15 (IIC Dr. Kuhn GmbH & Co KG):

B_0: 0,35 T
Core: ^{1}H
Resonance frequency: 15,1 MHz
Dwell time: 20 µs
Amount of data points: 1024
Measurement temperature: 80 °C
Hahn-echo p90°: 2,85 – 2,95 µs
p180°: 4,8 – 4,9 µs
τ: 30 ms
Repetition time: 300 - 350 ms
Measurement points 2D: 64
Repetition per point: 8

Compound Preparation

19 different Green Tire tread compounds were prepared with varying CBS and sulfur content (Tab. 1 and 2).

The mixing of the compounds followed a three-stage mixing process (Tab. 3). The curing times are depicted in Tab. 2.

Evaluation

For the evaluation, a Design of Experiment (DoE) approach was selected based on a special mixing design. To neglect the different total phr inside the different compounds, all amounts were considered in a relative way. The goal of this investigation was to answer the main question:

How well can CLD be described by a statistical model?

With the support of the DoE program, it was evaluated if a statistical model exists for the different investigated methods to determine the CLD. Tab. 4 shows the resulting correlation coefficients for each test method.

All methods show a high correlation coefficient besides swelling. This means that for all analytical test methods besides swelling a statistical model can be calculated which describes in a very sufficient way the CLD. The measurement

2 Varying CBS and sulfur contents

Sample no.	R2	R3	R4	R5	R6	R7	R8	R9	R10
sulfur/phr	4,15	4,15	1,79	0,23	0,20	2,18	1,79	4,15	0,99
CBS/phr	0,71	0,71	3,18	5,15	4,65	2,17	3,18	1,23	3,91
Curing time/min	60	60	15	60	60	15	15	60	20

Sample no.	R11	R12	R13	R14	R15	R16	R17	R18
sulfur/phr	0,99	1,53	4,15	4,15	2,97	2,84	2,97	0,20
CBS/phr	3,91	3,84	0,20	0,20	1,69	2,53	1,69	4,15
Curing time/min	20	15	60	60	30	30	30	60

EV System

CV System

3 Mixing process for the Green Tire compounds

stage and time	action
1st stage min: sec	fill factor 0,73; 70 rpm; chamber temperature: 70°C measured temperature: 130 -150°C
00:00 - 00:15	polymer
00:15 - 00:45	1/3 silica; 1/3 silane
00:45 - 01:15	1/3 silica; 1/3 silane
01:15 - 02:15	a) oil adsorbed on CB in a PE pouch b) 1/3 silica; silane c) protector
02:15 - 04:15	ZnO, stearic acid; Vulkanox HS; Vulkanox 4020;
04:15	dump & control temperature 45 s on open mill (4 mm nip), sheet out weigh compound for 2nd step; storage for 24 h / RT
2nd stage min: sec	fill factor 0,70; 70 rpm; chamber temperature: 90°C measured temp.: 130 -150°C
00:00 - 01:00	plasticize 1st stage
01:00 - 03:00	DPG; mix;
03:00	dump & control temperature 45 sec. on open mill (4 mm nip), sheet out weigh compound for 3rd step; storage for 4 - 24 h / RT
3rd stage min: sec	fill factor 0,68; 55 rpm, chamber temperature: 50°C measured temperature: > 110°C
00:00 - 02:00	batch stage 2; accelerators; sulfur
02:00	dump batch; process on open mill 20 sec. with 3 - 4 mm nip cut 3 x left, 3 x right with 3 mm nip roll up & pass through a 3 mm nip x 3 sheet off; store for minimum 12 h before vulcanization

4 Evaluation of crosslink methods

	R^2
Mooney-Rivlin	0,97
Thiol-Amine S_x	0,99
^{1}H-NMR	0,98
TSSR - Brabender - Modified by Heinz*	 0,98 0,99
Swelling	0,77
Multihysteresis - Entanglement module G_e - Network node module G_c - Strength of the soft bonds - Strength of stiff bonds - Relative cluster size - Filler volume relationship	 0,99 0,99 0,99 0,99 0,99 1

*: evaluation further optimized by Guth-Gold approach

error of swelling experiments is much higher than for all other measurements which leads to this low index.

A linear model was chosen for all static measurements like Mooney-Rivlin, Swelling, Thiol-Amine method, TSSR, Module Entanglements G_e, Module Crosslinks G_c, strength of weak bonds and strength of rigid bonds. A cubic model, which contains more influencing parameters, fits

5 Comparison of methods (Minimizing Standard Deviation)

Response	Name	Units	Obs	Analysis	Std. Dev.	Model
R50	Multihysterese filler volume ratio Φ_{eff}		16	Polynomial	0,04	Cubic
R45	Multihysterese Modulus crosslinks G_c	MPa	17	Polynomial	0,06	RCubic
R44	Multihysterese modulus entanglements G_e	MPa	17	Polynomial	0,22	RCubic
R8	NMR/t_{21}	s	18	Polynomial	0,34	RCubic
R49	Multihysterese medium rel. Cluster size x_0		17	Polynomial	1,24	Cubic
R47	Multihysterese strength weak bonds s_d	MPa	17	Polynomial	4,27	RQuadratic
R48	Multihysterese strength stiff bonds s_v	MPa	17	Polynomial	6,44	RQuadratic
R46	Multihysterese distance two entangiements n		17	Polynomial	10,27	RCubic
R3	TSSR/L	mol/m³	18	Polynomial	12,96	RCubic
R2	TSSR/Brabender	mol/m³	18	Polynomial	22,98	RCubic
R4	TSSR/Heinz	mol/m³	18	Polynomial	31,39	RCubic
R1	Mooney Rivlin	mol/m³	18	Polynomial	69,72	Linear
R5	Quellung Summe	mol/m³	18	Polynomial	84,61	RCubic
R7	Quellung S_1	mol/m³	18	Polynomial	89,94	Quadratic
R6	Quellung $S_1 + S_2$	mol/m³	18	Polynomial	90,56	Quadratic

↑ Observation: max. 18 samples were considered

better for all dynamic measurements like distance between two entanglements, relative cluster size x_0, and filler volume relationship Φ_{eff} (Tab. 5).

Knowing that different analytical test methods are suitable to describe the CLD, it was further evaluated how well the different single test methods correlate with each other. Tab. 6 gives an overview of the correlation coefficients between different methods.

All methods show very good correlation coefficients. Normally, this is a very good result, but in this case, there are also correlations between parameters which should NOT correlate with each other. The Thiol-Amine method should detect S_1, S_2 and the total S_x value. These three values should be independent from each other. To have a more detailed look, the calculated absolute CLD values from the thiol-amine method were compared with the values from the NMR analysis dependent on the sulfur content (Fig. 16) and additionally with each other (Fig. 17).

There is the expected tendency that a higher sulfur content leads indeed to a higher CLD (Fig. 16). But the comparison of S_1, S_2 and the total S_x value (Fig. 17) shows again this illogical behavior. For some marked samples, the S_1 content is even higher than the total S_x value which is impossible. To show this tendency clearer, Fig. 18 depicts the S_1, S_2 and the total S_x values for some selected samples, Tab. 7 the mean values of the standard deviation for all three measurements of the Thiol-Amine method.

All values in Fig. 18 are very similar, sometimes, as announced before, the S_1 content is higher than the total S_x value. There are three possible explanations for this:

- Only S_1 crosslinks are present, S_1 and S_x are identically considering the measurement error
- The Thiol-Amine method itself leads to a change in the network structure
- The Thiol-Amine combination does not react in the presence of silica with poly- and disulfidic bridges quantitatively

The first explanation seems illogical, a higher sulfur content should always lead to a higher amount of S_2 and polysulfidic bonds. This is well described in the literature 14.

To analyze if the second or the third reason delivers a plausible explanation the proposed mechanism [13] of the Thiol-Amine method is investigated in more detail. A selective cleavage of the sulfur chains is assumed (Fig. 19):

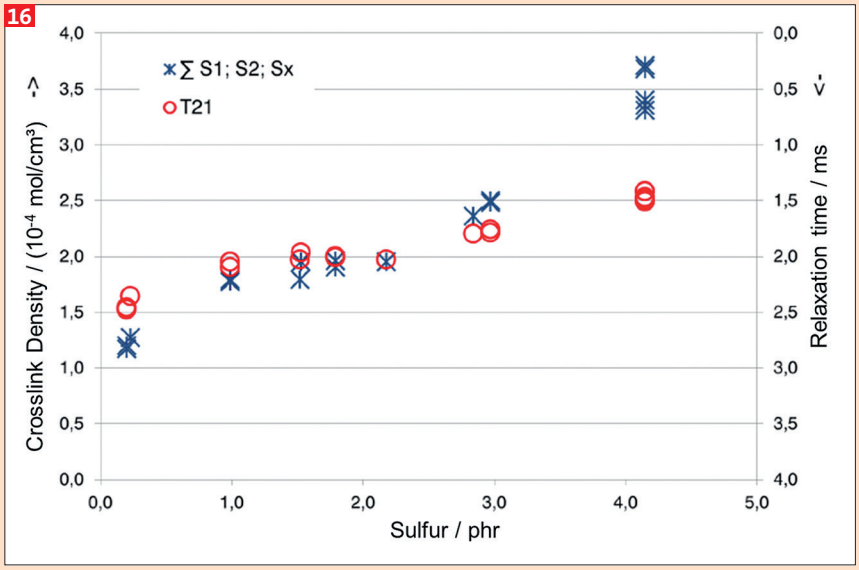

Fig. 16: ^{1}H NMR versus Thiol-Amine Method.

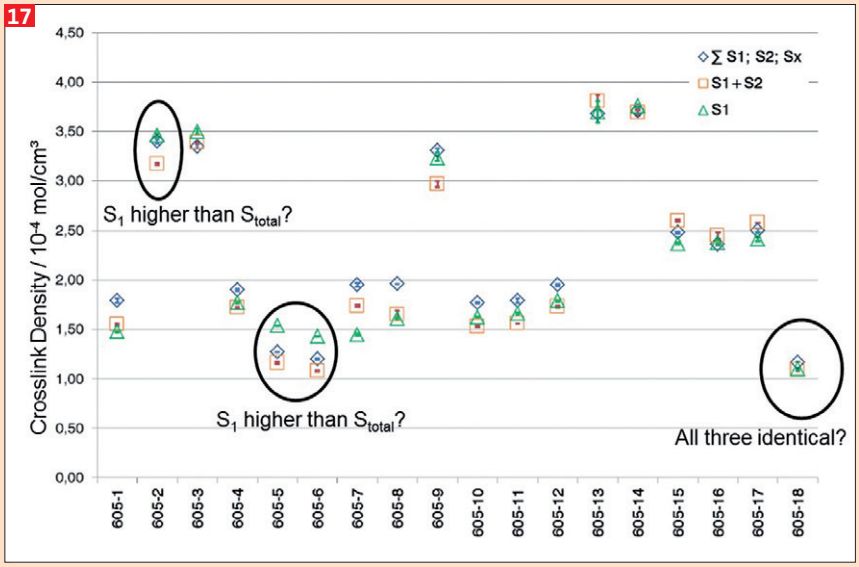

Fig. 17: Thiol-Amine Method: S_1, S_1+S_2, $\Sigma S_1+S_2+S_x$.

6 Correlation coefficients between different methods

	Thiol Amine $S_1 + S_2$	Thiol Amine S_1	Mooney-Rivlin	TSSR „Brabender“	TSSR „Heinz“
r^2 for Thiol-Amine Stotal	0.99	0.98	0.96	0.91	1.00
r^2 for Thiol-Amine $S_1 + S_2$		0.98	0.96	0.88	0.98
r^2 for Thiol-Amine S_1			0.97	0.84	0.96
r^2 for Mooney-Rivlin				0.82	0.95
r^2 for TSSR „Brabender					0.94
r^2 for TSSR modified by Heinz					0.94

But: Completely illogical correlation!

7 Swelling measurements (Thiol-Amine method) correlations

	Mean value of standard deviation / mol/m³
Swelling total	2,8
Thiol-Amine S_1+S_2	7,6
Thiol-Amine S_1	5,3

1. Cleavage of polysulfidic crosslinks: i-propane thiol and piperidine in n-heptane
2. Cleavage of di- and polysulfidic crosslinks: n-hexane thiol in piperidine

The Thiol-Amine combination gives an associate, possibly piperidinium propane-2-thiolate ion pair, in which the sulfur atom has enhanced nucleophilic properties. This is capable of cleaving organic trisulfides and higher polysulfides within 30 min at 20°C, while reacting with corresponding disulfides at about thousandth of this rate. The favored polysulfide cleavage can be explained by a $p_x - d_x$ delocalization of the displayed σ-electron pair of RSS- (Fig. 20).

This method works quite well in unfilled and CB filled rubber [13]. But what happens in the presence of silica? Or even more important, what happens in the presence of silica AND silane? There are different possible reactions which might occur:

→ Preferred coupling of hexanethiol or propanethiol to vinyl groups of polymers to create S_1?
→ Activation of unreacted Si 266™ to couple to the polymer?
→ Interaction with hexanethiol / propanethiol or piperidine with remaining silanol groups of the silica?

The first possibility would result in a coupling of hexane thiol or propane thiol to vinyl groups of the polymer. Due to the fact that this coupling would lead to additional pending groups which does NOT contribute to the CLD, this reaction might occur. It would consume hexane thiol or propane thiol which cannot participate anymore in the cleavage of the sulfur chains.

The second possibility contains the idea to activate remaining Si 266TM via piperidine which might lead to an additional silica-silane-polymer coupling. If this reaction occurs the CLD would be increased.

The third possibility includes two options: An interaction via hydrogen bonds from the thiol group to the silanol groups. The S...H bond is weaker than an O...H bond, therefore, it can be expected, that only a weak adsorption of hexane thiol or propane thiol at the silica surface occurs. The other option is the adsoption of piperidine at the remaining silanol groups of the silica. Piperidine as a basic substance should have high attractive forces to couple to the acidic silanol groups, therefore, this coupling is very likely. If the piperidine is adsorbed at the silica surface, it cannot activate anymore the hexane thiol or propane thiol to form the required active R-S-. Without this formation, a cleavage of poly- or disulfidic bridges is not possible anymore.

The last two possibilities would explain why the S_1 content is higher or at the same level than the sum from S_x, S_2 and S_1. But one more point has to be considered: For the cleavage of the disulfidic bonds, piperidine was used as a solvent. This should lead to a surplus in piperidine which means that the above considered conclusion can be mainly valid for the cleavage of the polysulfidic bonds where piperidine is used in smaller amounts. To clarify this finally, further investigations are required. But it seems to be most likely that the Thiol-Amine method is NOT applicable for the investigated silica-filled Green Tire tread system to determine S_1 and S_2. This has to be further evaluated, by varying e.g. the type and amount of silica, the type and amount of silane and the type and amount of accelerators.

18

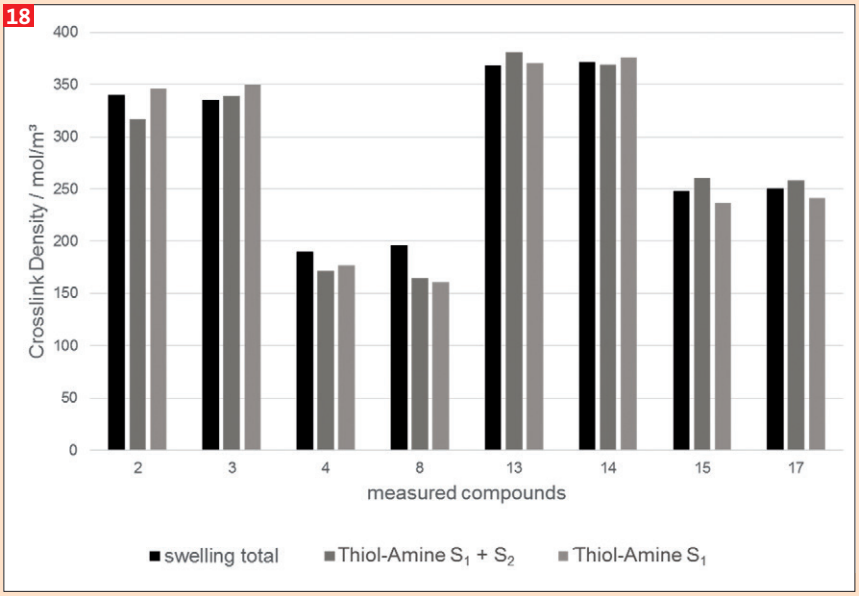

Fig. 18: Swelling measurements (Thiol-Amine method) correlations.

19

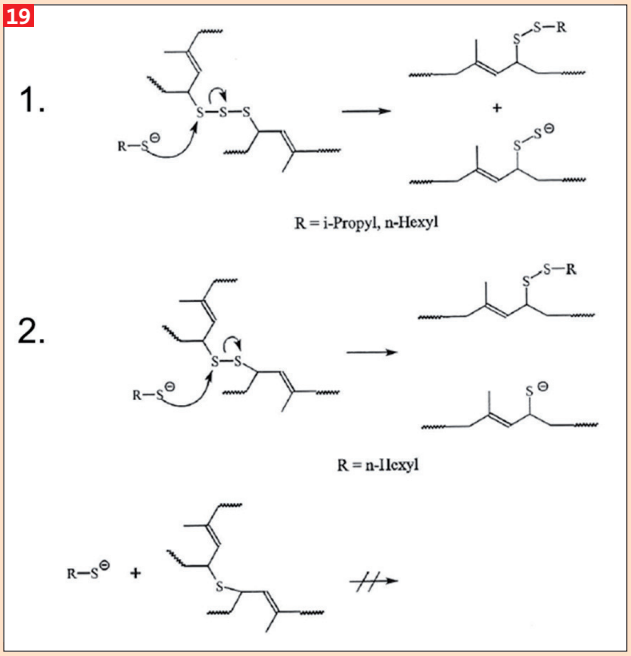

Fig. 19: Proposed mechanism for the thiol-amine reaction [13].

20

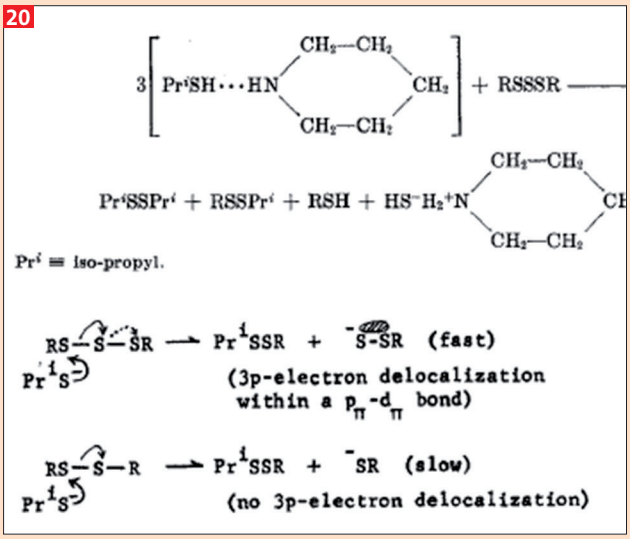

Fig. 20: Proposed mechanism for the Thiol-Amine reaction including the role of piperidine [13].

21

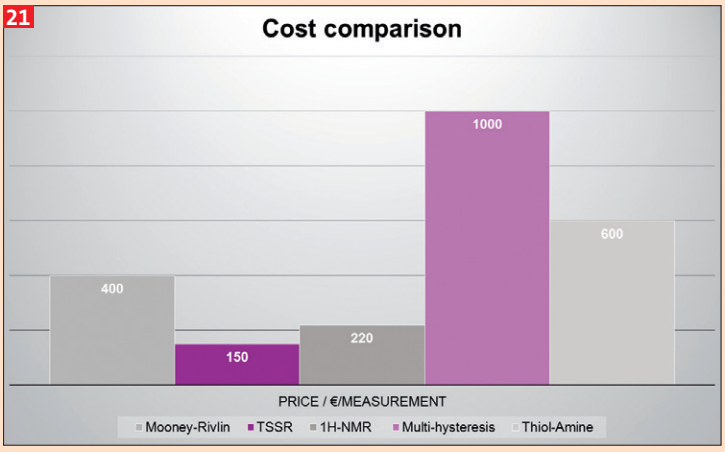

Fig. 21: Cost comparison.

Summary

All investigated test methods are suitable for a determination of the CLD. For the whole investigation series, it has to be considered that silica-filled rubber samples were investigated. The measurement of the CLD is not only influenced by the presence of the filler but also, in the case of using a silica/silane system, by the combination of polymer-polymer bonds and silica/silane/polymer bonds.

The standard deviation of the statistical models to predict the CLD is for the DFM and NMR the best, followed by TSSR. The swelling method contains a higher measurement error and delivers therefore a less significant statistical model. The Thiol-Amine method for S_1 and S_1+S_2 is not applicable in Green Tire tread compounds, an explanation for this is proposed. Taking finally the price into account, the TSSR is the cheapest method (Fig. 21), followed by NMR and Mooney-Rivlin.

Acknowledgement

The main author would like to thank Dr. Alexander Koepfer and Dr. Julia Hermeke for the intensive discussion about the Thiol-Amine method and Dr. Michael Heinz for providing the TSSR results. Furthermore, a special thank to the German Institute of Rubber Technology (DIK) in Hanover, Germany for performing the DFM, NMR and thiol-amine-measurements.

References

[1] B. A. Dogadkin, Vulcanization of Elastomers, Chemistry of Elastomers, 1st ed.; WNT: Warsaw, Poland (1976) 201.
[2] R. N. Datta, Rubber Curing Systems. Smithers Rapra Publishing **12** (2001).
[3] C. P. Rader, Vulcanization of Rubber – A. Sulfur and Non-Peroxides, Basic Elastomer Technology, 1st ed.; K. C. Baranwal, H. L. Stephens, Eds. Rubber Division: Akron, OH, USA (2001) 165.
[4] A. Y. Coran, Vulcanization, The Science and Technology of Rubber, 4th ed.; J. E. Mark, B. Erman, M. Roland, Eds. Academic Press (2013) 337.
[5] G. Heideman, R. N. Datta, J. W. M. Noordermeer, B. van Baarle, RUBBER CHEM. TECHNOL. **77** (2004) 512.
[6] N. J. Morrison, M. Porter, RUBBER CHEM. TECHNOL. **57** (1984) 63.
[7] J. L. Koenig, RUBBER CHEM. TECHNOL. **73** (2000) 385.
[8] M. Porter, The Chemistry of the Sulfur Vulcanization of Natural Rubber, The Chemistry of Sulfides, A. V. Tobolsky, Ed. Interscience: New York, NY, USA (1968) 165.
[9] J. V. Aleman, A. V. Chadwick, J. He, M. Hess, K. Horie, R. G. Jones, P. Kratochvil, I. Meisel, I. Mita, G. Moad, S. Penczek, R. F. T. Stepto, Pure Appl. Chem. **79** (2007) 1801.
[10] A. V. Chapman, M. Porter, Sulphur Vulcanization Chemistry, Natural Rubber Science and Technology, A. D. Roberts, Ed. Oxford Science Press: Oxford, UK (1988) 511.
[11] D. S. Campbell, A. V. Chapman, J. Nat. Rubb. Res. **5** (1990) 246.
[12] G. M. Bristow, R. F. Tiller, Kautsch. Gummi Kunstst. **23** (1970) 55.
[13] B. Saville, A. A. Watson, RUBBER CHEM. TECHNOL. **40** (1967) 100.
[14] K. S. Bandzierz, L. A. E. M. Reuvekamp, J. Dryzek, W. K. Dierkes, A. Blume, D. M. Bieliński, RUBBER CHEM. TECHNOL., DOI: 10.5254/rct.18.82685.
[15] A. Hasse et al, Kautsch. Gummi Kunstst. 55, **5** (2002) 236.
[16] M. Mooney, J. Appl. Phys. 11 (1940) 582
[17] R.S. Rivlin, Phil. Trans. Royal Soc. **A 241** (1949) 279.
[18] L.R.G. Treloar, The Physics of Rubber Elasticity, 3rd Edn., Clarendon Press, Oxford (1975)
[19] S. C. George, K. N. Ninan, S. Thomas, Polym. Polym. Compos. **7** (1999) 343.
[20] Fwata, I; Kimwa, S. I.; Iwawa, I: "Physical Constants of Rubbery Polymers", in Polymer Handbook, 4th edition, New York (1999)
[21] H. Lorenz, M. Klüppel, G. Heinrich: ZAMM **92**, 8 (2012) 608.
[22] N. Vennemann; TSSR, a Versatile Test Method For Thermoplastic Elastomers (TPE) and Rubber; Visit of Prince of Songhkla University, Thailand (2011).
[23] N. Vennemann, M. Wu, M. Heinz, Rubber World 246, **3** (2012) 18.
[24] M.M. James, E. Guth; J. Chem. Phys. **21** (1947) 237.
[25] P.J. Flory; J. Chem. Phys. **18** (1950) 108.
[26] A. Einstein, Analen der Physik **19** (1906) 289
[27] A. Einstein, Analen der Physik **34** (1911) 591
[28] F. Fuchs, Kautsch. Gummi, Kunstst. **59** (2006) 302.
[29] M. Heinz, N. Vennemann, M. Wu: 4th Rubber Symposium of the Countries of Danube. Oktober (2016).
[30] W. Gronski, RUBBER CHEM. TECHNOL65 (1992) **63.**